ELSEVIER

Surface Science 425 (1999) 141–151

surface science

Ordering and stabilization of C_{60} films on the $(\sqrt{3}\times\sqrt{3})R30^\circ$ Sn/Pt(111) surface alloy

Nathan Swami [a], Hong He [b], Bruce E. Koel [a,b,*]

[a] *Department of Materials Science, University of Southern California, Los Angeles, CA 90089-0482, USA*
[b] *Department of Chemistry, University of Southern California, Los Angeles, CA 90089-0482, USA*

Received 25 August 1998; accepted for publication 24 November 1998

Abstract

The deposition and growth of C_{60} on the $(\sqrt{3}\times\sqrt{3})R30^\circ$ Sn/Pt(111) surface alloy is compared with that on the Pt(111) surface at submonolayer, monolayer and multilayer coverages. We find that alloying Pt(111) with Sn arrests the charge transfer from Pt to adsorbed C_{60}, as seen from the absence of a shift in the $T_{1u}(1)$ vibrational levels of C_{60} probed by high resolution electron energy loss spectroscopy (HREELS). From low energy electron diffraction (LEED) observations it is determined that whereas ordering and graphitization of C_{60} on Pt(111) take place at 900 K, graphitization of C_{60} is inhibited by Sn alloyed into Pt(111). The rotated hexagonal LEED pattern of the ordered C_{60} monolayer is stabilized by the presence of Sn on Pt(111) until 1100 K, which is close to the fragmentation temperature of solid C_{60}. Upon heating C_{60} films on the $(\sqrt{3}\times\sqrt{3})R30^\circ$ Sn/Pt(111) surface alloy, Sn is dealloyed at about 500 K, and this dealloyed Sn reacts with C_{60} at 450–700 K, possibly resulting in polymerization. Auger electron spectroscopy annealing studies and the rise in intensity of the unpolarized Raman-active $A_g(2)$ mode at 1467 cm^{-1} support this conclusion. High temperature fragmentation of C_{60} in the presence of Sn leads to HREELS peaks at 250 and 740 cm^{-1}, prior to the formation of graphite.

Keywords: C60 films; Sn/Pt(111); Vibrational spectra

1. Introduction

The growth of ordered C_{60} films by modification of the substrate surface has been the objective of many recent studies [1–5]. Ordered C_{60} films have enhanced conductivity and stable electrical properties [6]. This is of importance particularly in the light of the interesting electrical properties of C_{60} [7], doped fullerides [8], and superfullerides [9], which may find applications in electrical devices [10]. Charge transfer interactions between C_{60} and metal [11–13] and semiconductor substrates [14] have been of great interest in light of understanding adsorbate–substrate bonding, and also in explaining the anomalous conductivity of C_{60} on some metal surfaces [15,16]. On Pt(111), C_{60} grows as a disordered film at 300 K because of strong chemisorption [17] that leads to low adsorbate mobility on the surface [5]. It has been proposed that annealing to 900 K enhances the adsorbate mobility and results in an ordered C_{60} film, as seen by the appearance of C_{60} domains in low energy electron diffraction (LEED) of C_{60}/Pt(111) [17,18]. However, since Pt(111) catalyzes the graphitization of C_{60} at 900 K, graphite domains

* Corresponding author. Fax: +1-213-740-3972.
E-mail address: koel@chem1.usc.edu (B.E. Koel)

0039-6028/99/$ – see front matter
PII: S0039-6028(98)00905-4

appear along with C_{60} domains in the LEED results [17], and the integrity of C_{60} in these films is uncertain.

In previous studies it was found that the alloying of Pt(111) with Sn to form the $(\sqrt{3}\times\sqrt{3})R30^\circ$ Sn/Pt(111) surface alloy [19] (henceforth called the $\sqrt{3}$ alloy), chemically deactivates Pt(111) [20]. The main objective of this work was to chemically modify the Pt–C_{60} interface by alloying Pt(111) with Sn, and study the deposition and growth of ordered C_{60} films on this less reactive alloy surface. We find that Sn arrests the charge transfer from Pt(111) to C_{60} on deposition at 300 K. Upon annealing C_{60} on the $\sqrt{3}$ alloy to higher temperatures, we find that Sn inhibits graphitization of C_{60} on Pt(111) in the 900–1100 K temperature range, such that ordering of C_{60} occurs on this alloy surface without decomposition. To date, no studies of C_{60} growth on bimetallic alloy surfaces have been reported and hence this work provides a useful reference for future studies in this field.

The interaction of Sn with C_{60} is also of interest. Superconductivity up to 37 K of Sn-doped C_{60} has been reported [21]. Vibrational studies of this compound have identified features in the spectra that differ distinctly from that of pristine C_{60} [22]. Further, the resistivity of C_{60} films is known to drop sharply in the presence of an Sn layer [23]. Whereas photoemission spectroscopy results [24] suggest no charge transfer interactions between Sn and C_{60}, both absorption and luminescence studies [25] show absorption band broadening and new bands of the C_{60} film attributed to Sn intercalation. The structure and properties of the Sn-doped C_{60} phase have not been studied. It has been suggested that the reaction of Sn with C_{60} is slow and limited by diffusion of Sn into the C_{60} lattice [24]. In previous studies, the Sn-doped phase was usually present with an excess amount of pristine C_{60}, and this complicated interpretation of results. This is especially true when using surface-sensitive probes, such as photoemission for fulleride films [26]. A related objective of the work reported herein was to study the interaction of only a few monolayers of C_{60} with Sn from the $\sqrt{3}$ surface alloy, in order to minimize the effects of unreacted C_{60} on the results.

Homogenous decomposition of C_{60} molecules in the gas phase [27] and solid phase [28,29] at high temperatures has been studied. Isolated C_{60} molecules fragment at 1700 K and this is lowered to about 1200 K for solid C_{60} [28,29]. Although the onset temperature for fragmentation of 1 ML C_{60} on various metal surfaces is difficult to ascertain, extensive decomposition of C_{60} clearly occurs by 900 K on Pt(111) [17] and 850 K on Ni(110) [18] and Rh(111) [13]. No intermediates were identified in the vibrational spectra of the conversion of C_{60} to graphite on Pt(111), Ni(110) or Rh(111). In the current study, Sn on Pt(111) stabilizes the ordered C_{60} monolayer until 1100 K, and graphitic domains appear in LEED only at 1200 K. In order to characterize any intermediates in the decomposition of C_{60} to graphite, this work presents vibrational spectra of C_{60} films annealed to 1200 K on the $\sqrt{3}$ alloy surface.

2. Experimental methods

The experiments were conducted in a three-level ultrahigh-vacuum chamber with a base pressure of 2×10^{-10} Torr, as has been described previously [17]. The top level was equipped with a double-pass cylindrical mirror analyzer (CMA) which was used for Auger electron spectroscopy (AES), X-ray photoelectron spectroscopy (XPS) and ultraviolet photoelectron spectroscopy (UPS). The middle level was equipped with LEED optics and a quadrupole mass spectrometer (QMS) for temperature-programmed desorption (TPD) studies. The bottom level contained an LK2000 spectrometer for high resolution electron energy loss spectroscopy (HREELS). The Pt(111) crystal was mounted on two vertical Ta rods which were imbedded in liquid-nitrogen-cooled copper blocks at the bottom of a differentially pumped *XYZ*-manipulator. A chromel–alumel thermocouple was spot-welded directly to the edge of the crystal, and accuracy of the temperature measured was within 5 K, as checked by TPD of CO/Pt(111) for temperatures below 600 K and by an optical pyrometer for temperatures above 800 K. The sample could be cooled to 90 K or resistively heated to 1200 K. The Pt(111) sample was cleaned by a standard combination of Ar^+ ion sputtering at $P_{Ar}=5\times10^{-5}$ Torr with a beam voltage of 800 V, annea-

ling to 800 K in 5×10^{-8} Torr O_2 and flashing to 1200 K in vacuum. Sample cleanliness was checked with AES, LEED and HREELS.

AES data were obtained using an incident beam energy of $E_p=3$ keV and at a resolution of 0.6% of the kinetic energy, with the incident electron beam current reduced to 1 μA to minimize electron beam damage of C_{60}. XPS data were obtained using Mg Kα X-rays (1253.6 eV) with the CMA operated at 25 eV pass energy (resolution: 400 meV) to give an FWHM of 1.5 eV for the Pt ($4f_{7/2}$) peak. All binding energies (BEs) were referenced to that of the Pt($4f_{7/2}$) level at 71.2 eV BE. The HREELS spectra were recorded in the specular direction at an angle of 60° from the surface normal and a primary beam energy of 4.5 eV.

The overall energy resolution of the spectrometer was about 50 cm^{-1}, and the count rates at the elastic peak were about 100 kHz for clean Pt(111). The spectra were normalized to the intensity of the elastic peak.

C_{60} (99.9% purity, MER Corp.) was evaporated from a Ta boat on to the Pt(111) or the $(\sqrt{3}\times\sqrt{3})$R30° Sn/Pt(111) surface alloy at 300 K. The absence of substantial hydrocarbon impurities from C_{60} deposition was confirmed by the absence of any detectable C–H stretching peak in HREELS. The $(\sqrt{3}\times\sqrt{3})$R30° Sn/Pt(111) surface alloy [19] was prepared by Sn deposition on Pt(111) at 300 K such that the AES signal intensity ratio for Pt(237 eV)/Sn(430 eV) was about 0.1, followed by a 950 K anneal for 30 s resulting in a clear $(\sqrt{3}\times\sqrt{3})$R30° LEED pattern and Pt(237 eV)/Sn(430 eV) = 0.4. The amount of C_{60} dosed to the surface was determined by assigning the deposition time required to form 1 ML C_{60} from the first 'break' in the AES uptake curve of C_{60} [17] on the various substrate surfaces. An upper limit for the C_{60} coverage in the monolayer on Pt(111) would be given by an hcp monolayer with 1.15×10^{14} molecules/cm^2 or $\theta(C_{60})=0.1$ relative to the Pt(111) surface atom density.

3. Results

3.1. Adsorbate–surface charge transfer interactions

HREELS spectra for adsorption of C_{60} on Pt(111) and the $\sqrt{3}$ alloy at 300 K are shown in Figs. 1 and 2 respectively. Multilayer C_{60} films (5 ML) on Pt(111) in Fig. 1 showed dipole-active peaks at 533 cm^{-1} [$T_{1u}(1)$], 1215 cm^{-1} [$T_{1u}(3)$] and 1467 cm^{-1} [$T_{1u}(4)$], whereas the dipole inactive $H_g(4)$ mode appeared at 756 cm^{-1} [30–32]. The peak for the $T_{1u}(1)$ mode shifted from 511 cm^{-1} at $\theta(C_{60})=0.3$ ML to 533 cm^{-1} at $\theta(C_{60})=5$ ML. The shift of this vibrational mode has been correlated in theoretical [30] and experimental studies [31,32] to adsorbate–surface charge transfer interactions, with an attribution that the $T_{1u}(1)$ mode exhibits a roughly linear shift of −1.25 meV (−10 cm^{-1}) per electron transferred to C_{60} [31]. The spectra in Fig. 1 indicate, on this basis, that about two electrons are transferred per C_{60} molecule at $\theta(C_{60})=0.3$ ML and that one electron is transferred per C_{60} molecule at $\theta(C_{60})=1$ ML. This charge transfer interaction accompanies strong chemisorption bonding of C_{60} to the surface and leads to the growth of a disordered C_{60} film [5,17]. Arresting charge

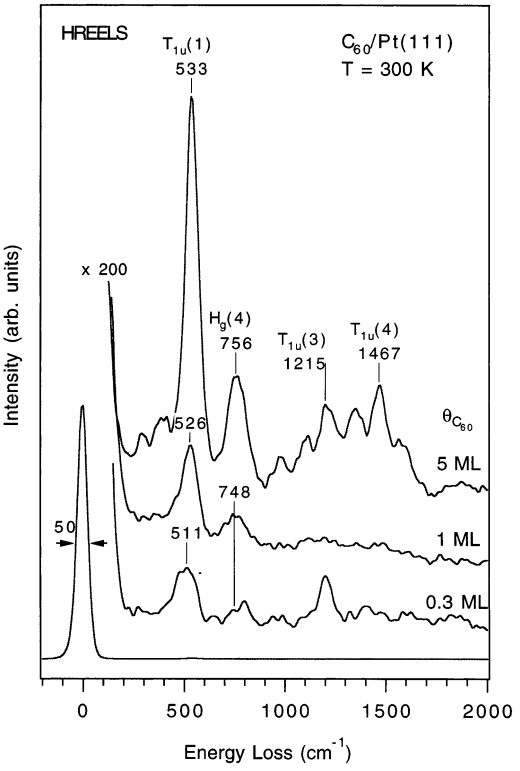

Fig. 1. HREELS spectra of C_{60} deposited on Pt(111) at 300 K.

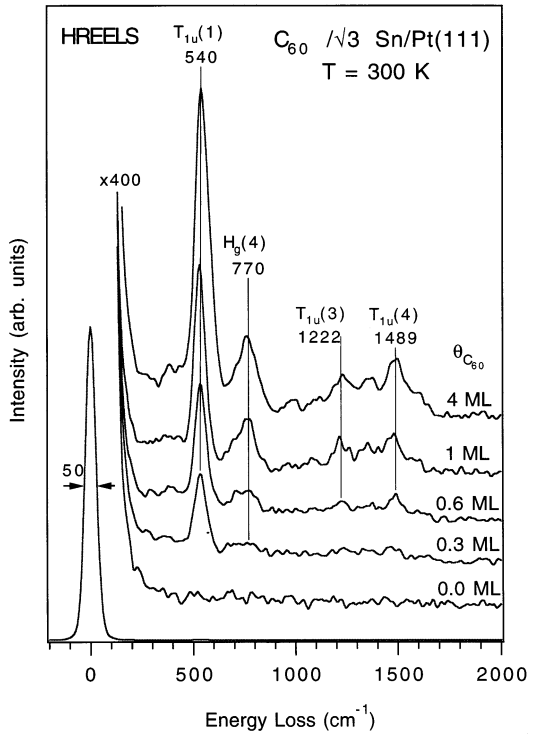

Fig. 2. HREELS spectra of C_{60} deposited on $(\sqrt{3}\times\sqrt{3})R30^\circ$ Sn/Pt(111) surface alloy at 300 K.

transfer from the surface to the C_{60} molecule weakens the chemisorption bond and leads to enhanced adsorbate mobility that results in ordering of the C_{60} film [5]. The results in Fig. 2 for the growth of C_{60} on the $\sqrt{3}$ alloy surface showed that the $T_{1u}(1)$ mode exhibited no discernible shift from submonolayer to multilayer coverages. This demonstrates that alloying Pt(111) with Sn arrests charge transfer from the surface to the C_{60} molecule.

3.2. *Growth of ordered C_{60} films*

The growth of ordered C_{60} films on Pt(111) may be accomplished by annealing multilayer C_{60} films to temperatures between 900 and 1000 K. The resulting LEED pattern corresponds to two hexagonal domains rotated by $29\pm3^\circ$, as reported and discussed previously [18]. Fig. 3a and b shows our LEED observations after annealing multilayer C_{60} films (5 ML) on Pt(111) in this temperature

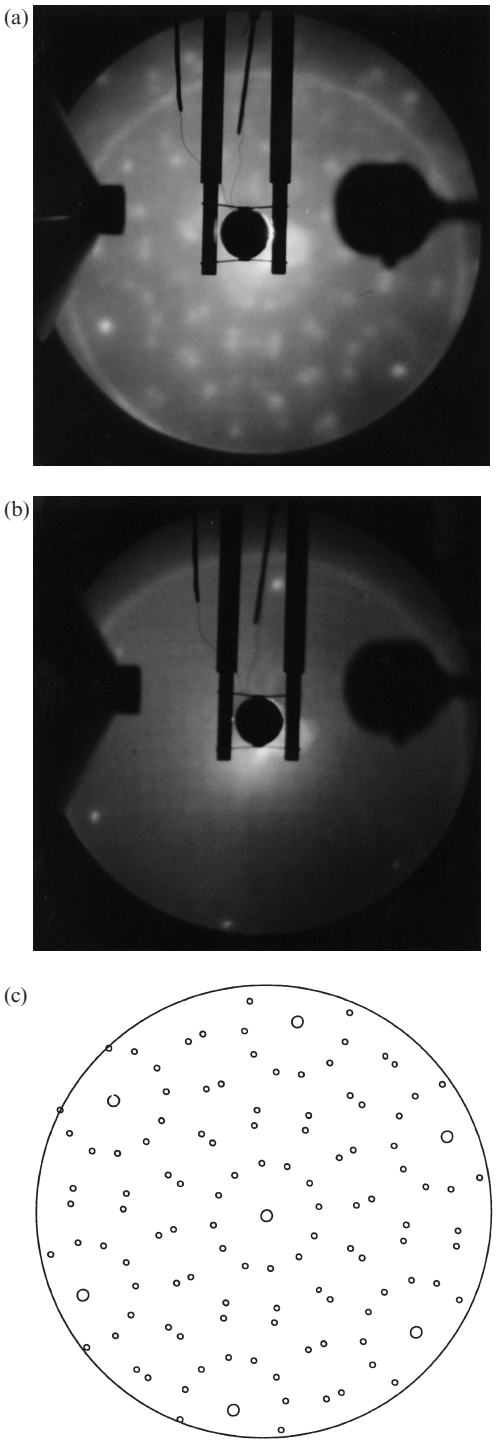

Fig. 3. LEED observations for C_{60} films deposited on Pt(111) at 300 K, after heating to (a) 900 K, (b) 1000 K; (c) schematic explanation of the LEED [18]. All images are at $E_p=65$ eV.

range. Fig. 3c shows a schematic drawing of the C_{60} and Pt spots in the LEED patterns. The rotated hexagonal patterns appear in the images after heating to 900 K, and they merge into the diffuse background following heating to 1000 K. It is quite clear in the LEED images of Fig. 3 that a graphitic 'ring' appears around the (1×1) spots after the 900 K anneal, and this is the sole LEED feature after the 1000 K anneal. Our interpretation of these observations is that Pt(111) catalyzes the graphitization of C_{60} beginning at temperatures as low as 900 K.

Fig. 4 shows the LEED patterns seen after a multilayer C_{60} film (4 ML) was deposited and annealed on the $\sqrt{3}$ alloy surface in the same manner as described above for Pt(111). The two rotated hexagonal domains also appeared here after heating to 900 K, but without a graphitic ring around the (1×1) spots. Furthermore, this LEED pattern persisted even after heating to 1100 K. Upon annealing to 1200 K, the graphitic ring does appear along with very weak C_{60} domains. These results demonstrate that Sn deactivates Pt(111) for the graphitization of C_{60} and stabilizes the ordered C_{60} monolayer until 1100 K, which is close to the fragmentation temperature of solid C_{60} [28].

3.3. Interaction of Sn with C_{60}

The interaction of Sn with C_{60} was studied by heating 4 ML C_{60} films deposited on the $\sqrt{3}$ alloy surface ($\theta_{Sn}=0.33$ ML) at 300 K, to various temperatures up to 1200 K for 1 min. These films were then probed with AES, HREELS and XPS at 300 K. The results of the AES annealing studies are shown in Fig. 5. In the absence of C_{60}, the $\sqrt{3}$ alloy is stable until 1000 K, with Sn desorption and diffusion into the bulk occurring at higher temperatures, and causing a loss of the $(\sqrt{3}\times\sqrt{3})R30^\circ$ LEED pattern. At $T\geq1100$ K, excess Sn in the bulk segregates to the surface.

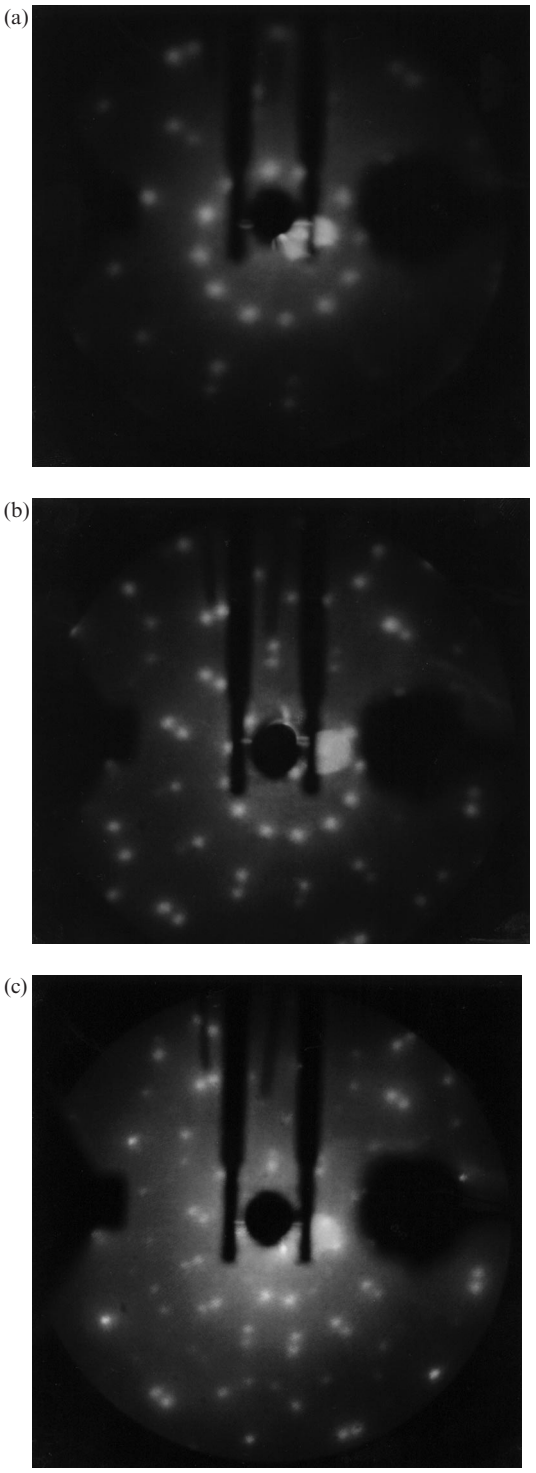

Fig. 4. LEED observations for C_{60} films deposited on the $(\sqrt{3}\times\sqrt{3})R30^\circ$ Sn/Pt(111) surface alloy at 300 K, after heating to 900 K. The LEED spectra were obtained at an E_p of (a) 25 eV, (b) 35 eV and (c) 65 eV. No change in the pattern occurs after heating up to 1100 K.

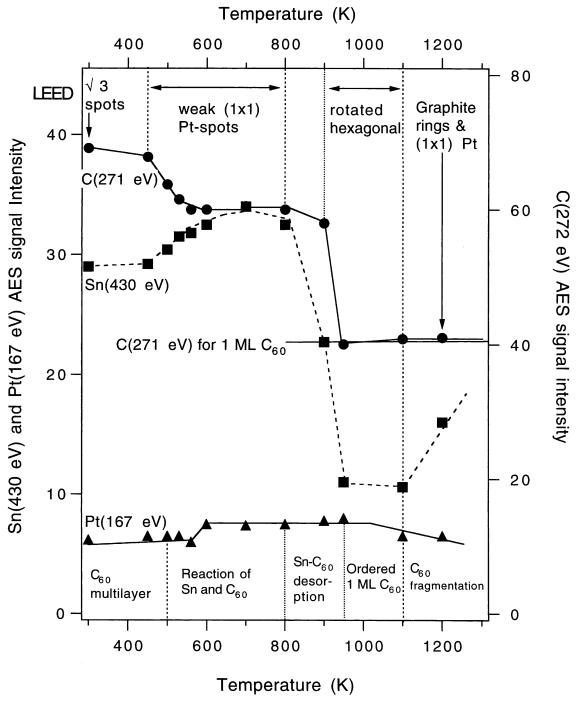

Fig. 5. AES studies of multilayer C_{60} films (4 ML) following annealing on the $(\sqrt{3}\times\sqrt{3})R30^{\circ}$ surface alloy in the 300–1200 K temperature range. LEED observations are given in the top panel, followed by corresponding AES intensities of the C(271 eV), Sn(430 eV) and Pt(167 eV) signals.

Multilayers of C_{60} desorb at 600 K [13], but the C_{60} monolayer either desorbs at 800 K, as on Au(110) [12], or graphitizes at 850 K, as on Ni(110) [18] and on Rh(111) [13]. For C_{60} on Pt(111), heating C_{60} multilayers above 600 K produces C_{60} coverages in excess of the monolayer value and graphitization of C_{60} begins at 900 K [17].

For C_{60} multilayers on the $\sqrt{3}$ alloy, as shown in Fig. 5, the C(271 eV) signal rapidly dropped between 450 and 600 K as a result of desorption of the C_{60} multilayer. Strong interactions with Sn from the $\sqrt{3}$ alloy arrest this drop and the C(271 eV) signal does not reach the C_{60} monolayer value [17] at the sublimation temperature of 600 K. After heating to 950 K, the C(271 eV) signal dropped to the monolayer value and remained at this value even after heating to 1200 K. The Sn(430 eV) AES signal intensity increases significantly after annealing at temperatures of 450–600 K, and reached a nearly constant value between 600 and 800 K. Upon heating to 900 K, a big drop in the Sn(430 eV) signal was seen, concomitant with the steep drop of the C(271 eV) signal to the C_{60} monolayer value at 900–950 K. From 950 to 1100 K the Sn(430 eV) signal was constant, but increased again after the 1200 K anneal (probably because of diffusion of Sn from the bulk of the Pt crystal to the surface). The Pt(167 eV) AES signal intensity rose between 500 and 600 K, because of desorption of the C_{60} multilayer and was more or less constant after 600 K; it then falls after heating to 1100 K, most likely because of diffusion of Sn to the surface. In the region between 450 and 600 K, desorption of the C_{60} multilayer and Sn diffusion to the surface take place, as seen by the decrease in the C(271 eV)/Pt(167 eV) ratio from 11.0 to 8.0 and the increase in the Sn(430 eV)/Pt(167 eV) ratio from 4.2 to 4.9. Between 600 and 800 K the C(271 eV)/Pt(167 eV) and Sn(430 eV)/Pt(167 eV) ratios were constant; however, between 800 and 950 K both Sn and C_{60} are lost from the surface, as seen by falls in the C(271 eV)/Pt(167 eV) ratio from 8.0 to 6.0 and the Sn(430 eV)/Pt(167 eV) ratio from 4.8 to 1.4. The C(271 eV)/Pt(167 eV) ratio was constant at 6.0 between 950 and 1200 K, indicating about 1 ML C_{60} surface coverage. The Sn(430 eV)/Pt(167 eV) ratio was constant at about 1.4 between 950 and 1100 K, and increased to 2.2 after heating to 1200 K, due to diffusion of excess Sn to the surface.

The LEED pattern over this temperature range, obtained under the same conditions as the AES data, is also indicated along the top panel of Fig. 5. At 300 K, the C_{60} multilayer is disordered and only the $\sqrt{3}$ alloy spots were observed. The $\sqrt{3}$ spots disappeared and only the (1×1) Pt spots were visible in the 500–800 K temperature range. This indicates that the $\sqrt{3}$ ordered surface alloy is destroyed in this temperature range in the presence of C_{60} on the surface and that no other ordered Sn/Pt(111) structure is formed. After annealing to 900 K, rotated hexagonal spots appeared, as described in Section 3.2, and these persisted until the 1100 K anneal. After annealing to 1200 K, a faint graphitic ring appeared around the (1×1) Pt spots with a large diffuse background.

One explanation of these results is that the doping of C_{60} with Sn begins at 450 K via interdiffusion of Sn and C_{60}. This explains the loss of the $\sqrt{3}$ Sn/Pt(111) spots with the rise of the Sn(430 eV) signal and fall of the C(271 eV) signal seen in Fig. 5 in the 450–600 K temperature range. This Sn-doped phase desorbs/decomposes near 900 K, leaving a 1 ML C_{60} film on a Pt(111) surface with reduced Sn concentration [compared with the $\sqrt{3}$ Sn/Pt(111) surface alloy]. The presence of Sn at the Pt(111) surface preserves the ordered C_{60} monolayer film, inhibiting graphitization until 1200 K.

The HREELS warm-up studies shown in Fig. 6 support this explanation. The dipole-active $T_{1u}(1)$, $T_{1u}(3)$ and $T_{1u}(4)$ modes of C_{60} appear at 540 cm^{-1}, 1222 cm^{-1} and 1489 cm^{-1} respectively for multilayer C_{60} films on the $\sqrt{3}$ alloy at 300 K. Annealing to 450 and 700 K increased the intensity of a new peak at 1467 cm^{-1}. We believe that this peak does not arise from the softening of the

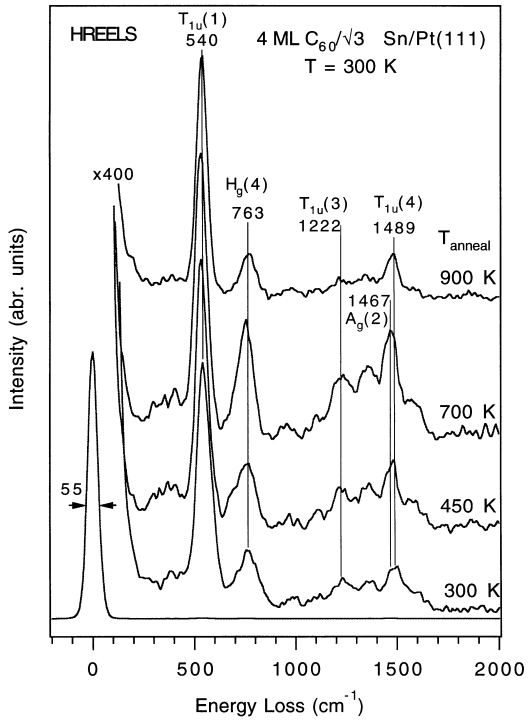

Fig. 6. HREELS spectra for 4 ML C_{60} deposited on $(\sqrt{3} \times \sqrt{3})R30°$ Sn/Pt(111) surface alloy at 300 K, following sequential annealing to temperatures up to 900 K.

$T_{1u}(4)$ mode, since it does not obey the expected intensity ratio of $T_{1u}(1):T_{1u}(2):T_{1u}(3):T_{1u}(4) = 100:29:6:5$, characteristic of the icosahedral symmetry of C_{60} [33]. This indicates that the icosahedral symmetry of the C_{60} molecule is destroyed in the presence of Sn on Pt(111) at 450–700 K. This 1467 cm^{-1} peak is similar to the peak at 1451 cm^{-1} in the FTIR spectrum after vapor deposition of Sn on C_{60} films, which was attributed to a Sn-doped C_{60} phase [22]. After a 900 K anneal, the peak in Fig. 6 at 1467 cm^{-1} is diminished and the characteristic vibrational features of C_{60} are regained. This indicates desorption and/or decomposition of the Sn–C_{60} phase. It is also seen that the peak for the $T_{1u}(1)$ mode, which is sensitive to charge transfer [1,2], shifted down from 540 cm^{-1} at 300 K to 533 cm^{-1} after heating to 450 and 700 K, but it regained its original value of 540 cm^{-1} after heating to 900 K. This shift indicates only a small charge transfer to the C_{60} molecule after heating to 450 and 700 K on the $\sqrt{3}$ surface alloy.

XPS was used to study the shift of the C(1s) and Sn(3d) levels. Fig. 7 compares spectra after deposition of a 4 ML C_{60} film on the $\sqrt{3}$ alloy surface at 300 K with those obtained by heating the film to 700 K where the surface coverage of C_{60} is decreased. In the spectra of Fig. 7a, the main C(1s) peak is fitted along with the expected satellite peak at 1.9 eV higher BE for the on-site molecular excitation across the HOMO–LUMO gap [34]. A downward shift of 0.30 eV was seen for the C(1s) level upon heating to 700 K.

This decrease in BE has been identified with charge transfer to C_{60} for 1 ML C_{60}/Cu(100) [35] and K-doped fullerides [36]. In the latter case, shifts in the K(2p) levels were also seen. Fig. 7b compares the Sn(3d) levels for a thick Sn film [10 ML Sn/Pt(111)] with those obtained after heating 4 ML C_{60} on the $\sqrt{3}$ alloy to 700 K (the Sn(3d) levels of the $\sqrt{3}$ alloy have the same BE as those of a thick Sn film [37]). Upon heating C_{60} films on the $\sqrt{3}$ alloy to 700 K, the Sn($3d_{5/2}$) level is shifted to higher BE by 0.1 eV, and the splitting between the Sn(3d) levels increased from 8.4 to 8.7 eV. Both the Sn($3d_{5/2}$) and Sn($3d_{3/2}$) levels were broadened and the Sn(3d) peaks could

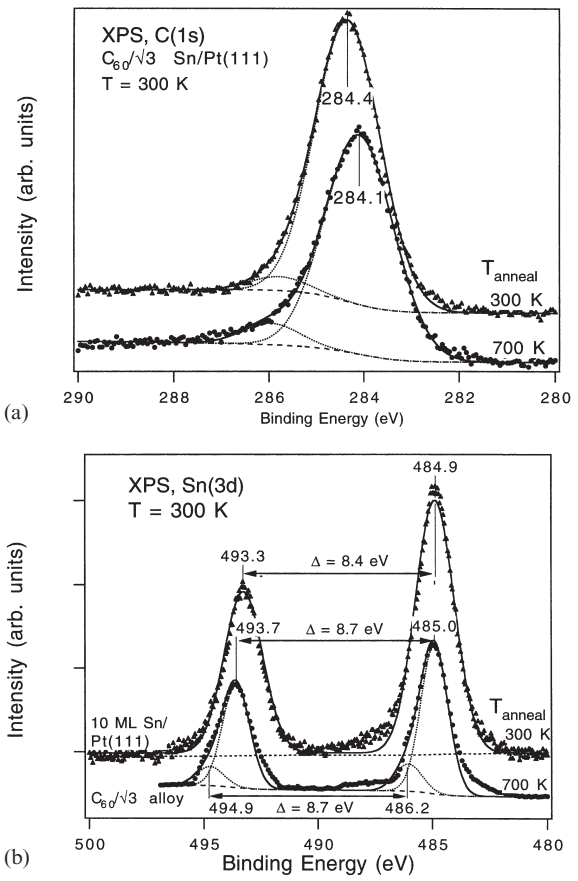

Fig. 7. XPS spectra of (a) C(1s) (b) Sn(3d) core levels, for 4 ML C_{60} deposited on $(\sqrt{3}\times\sqrt{3})R30^\circ$ Sn/Pt(111) surface alloy at 300 K, after annealing this film to 700 K. The C(1s) level shows a 0.3 eV chemical shift to lower BE. In comparison with thick Sn films, the Sn(3d) levels show some broadening, which causes small increases in BE and in the splitting of the levels.

be fit well by using two peaks of 1.5 eV FWHM. The high BE component shows a shift of 1.2 eV in both the $Sn(3d_{5/2})$ and $Sn(3d_{3/2})$ levels. This can be compared with a shift of 1.75 eV of the Sn(3d) levels on forming SnO_2 [38]. The proportion of this oxidized Sn species is quite small (about 15% of the total Sn). Because there are two forms of Sn present, it is difficult to determine the extent of charge transfer interactions between Sn and C_{60}. Covalent bonding of Sn and C_{60} could lead to a rearrangement of bonds in the compound that breaks the original icosahedral symmetry of the C_{60} molecule. Junzhou et al. [24] ruled out charge transfer interactions between Sn and C_{60}, and suggested that clathrate compounds are formed. This was based on the lack of changes in the photoemission spectra of pristine C_{60} in comparison with that of Sn on C_{60} films annealed to 573 K. We will return to discussion on this topic in Section 4.

3.4. High temperature annealing studies

The ordered C_{60} monolayer is maintained until 1100 K on the Sn/Pt(111) surface, and graphite domains only appeared in LEED after heating to 1200 K. HREELS studies after heating the ordered C_{60} monolayer on Sn/Pt(111) to 900–1200 K were performed in order to characterize intermediates leading to graphite. These spectra are shown in Fig. 8. The vibrational structure of the ordered C_{60} monolayer obtained after the

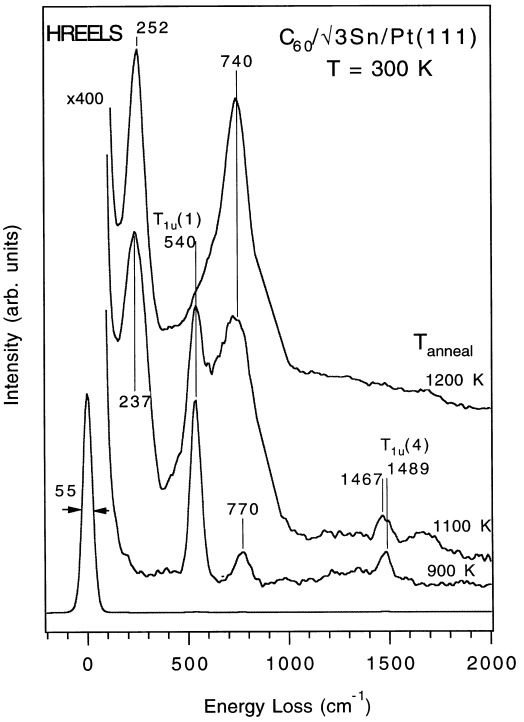

Fig. 8. HREELS spectra after high temperature annealing of the ordered C_{60} monolayer, produced by heating multilayer C_{60} films on the $\sqrt{3}$ Sn/Pt(111) surface alloy to 900 K. Extensive fragmentation of C_{60} occurs at $T \geq 1100$ K, and is nearly complete by 1200 K.

1100 K anneal is dramatically altered from that after the 900 K anneal. C_{60} features are still seen in the spectrum (consistent with the persistence of the rotated hexagonal LEED pattern), but large intensity changes start to take place in the spectra and new features appeared at 237, 740 and 1467 cm^{-1}. After a 1200 K anneal the C_{60} peaks are almost totally eliminated and only a shoulder was observed at 540 cm^{-1}. The new HREELS peaks shift to 252 and 740 cm^{-1}. We currently have no assignments of these new features. The above results may be contrasted with those obtained on heating C_{60} films on Pt(111) to 900–1200 K [17]. An ordered C_{60} adlayer with graphite domains was produced at 900 K, the ordered C_{60} domains were lost after 1000 K and graphitization was complete by 1050 K. Hence the new peaks in the HREELS of C_{60} films on the $\sqrt{3}$ alloy heated to 1100–1200 K are associated with the presence of Sn on Pt(111), and these peaks are enhanced at 1200 K because of Sn diffusion to the surface at these temperatures, as was shown by AES results.

4. Discussion

The alloying of Pt(111) with Sn to form the $(\sqrt{3}\times\sqrt{3})R30^{\circ}$ structure results in comparatively small electronic changes in the Pt valence band [37], and thus the influence of Sn on the chemistry of Pt(111) has been attributed mostly to site blocking effects that deactivate the surface for reaction with many organic molecules [39]. However, some electronic effect of alloyed Sn at the Pt(111) surface was also seen, for example in NO chemisorption studies on the $\sqrt{3}$ Sn/Pt(111) alloy [40]. In studies of ethylene chemisorption on the $\sqrt{3}$ alloy [39], backbonding interactions are reduced in comparison with that on clean Pt(111), and ethylene rehybridization towards sp^3 and di-σ bonding is also reduced. This is particularly relevant to the current study, where we propose that charge transfer from Pt(111) to C_{60} is inhibited by alloying Sn with Pt(111). The stabilization of the ordered C_{60} monolayer and the arresting of graphitization of C_{60} up to 1100 K, by deactivation of Pt(111) via alloying with Sn, is consistent with the chemistry observed for small organic molecules on this surface alloy.

From an analysis of the intercalation energies of various transition metals, alkaline earth metals and alkali metals in the C_{60} lattice, it was suggested [41] that most transition metals, including Sn, were unlikely to form intercalation compounds with C_{60} owing to their large cohesive energies. Yet, Zhao et al. [22] concluded that intercalation compounds of Sn and C_{60} are formed. The two chief observations concerning the interaction of Sn and C_{60} described in earlier work [21–25] were the development of new peaks in the 1450–1470 cm^{-1} region of the vibrational spectra and a drop in resistivity of C_{60} after interaction with Sn. The high electronegativity of Sn [42] compared with that of alkali and alkaline earth metals, with which C_{60} readily forms compounds, and the small amount of oxidized Sn observed in XPS are consistent with only a small charge transfer per C_{60} molecule from Sn. Covalent bonding between Sn and C_{60} would lead to rearrangement of bonds in C_{60} that break the original icosahedral symmetry of the molecule. Further, it is possible that Sn induces polymerization of C_{60}, as has been suggested to result from interaction of C_{60} with Pd [43], Ti [44] and Pt [17]. Peaks at 1450–1470 cm^{-1} in the FTIR spectrum were assigned previously [45,46] to the unpolarized Raman-active $A_g(2)$ mode of polymerized C_{60}. Our HREELS results are quite similar to this. Polymerization of C_{60} would also explain the air sensitivity of the 1451 cm^{-1} mode seen by Zhao et al. [22], since Eklund et al. [46] observed that oxygen intercalation into the C_{60} lattice reduced polymerization. Furthermore, polymerization shifts the valence band levels of C_{60} towards the Fermi energy [47], leading to increased emission at E_F. This latter effect may explain the drop in resistivity of C_{60} upon interaction with Sn.

Although the interaction of C_{60} with the $\sqrt{3}$ alloy surface at 300 K is weaker than on Pt(111), as seen by the lack of any adsorbate–surface charge transfer interactions, the interaction of C_{60} with dealloyed Sn is quite strong, as seen by the significant changes in the AES, LEED and

HREELS results for heating 4 ML C_{60} films on the $\sqrt{3}$ alloy to temperatures above 300 K. In the presence of C_{60}, dealloying of the $\sqrt{3}$ Sn–Pt alloy takes place at about 500 K, as seen by the disappearance of the $\sqrt{3}$ spots and the presence of only weak (1×1) Pt spots in LEED. Upon heating to 450–700 K, it is possible that dealloyed Sn induces polymerization of C_{60}. This would be consistent with the behavior of the $A_g(2)$ mode in HREELS and the concomitant Sn diffusion to the surface seen in AES. This would also explain the AES results, which indicate that the C_{60} coverage is stabilized at about 2 ML after heating a thicker film to 500–800 K and which then decreases to 1 ML C_{60} after heating to 900 K. Following heating to 900 K, the intensity of the $A_g(2)$ peak is diminished in HREELS, and Sn(430 eV) and C(271 eV) signals in AES drop to the respective values for 1 ML C_{60}, indicating the decomposition or desorption of the Sn-polymerized C_{60} phase. After heating to 900–1100 K the surface is composed of an ordered C_{60} monolayer film, as deduced by LEED and AES. Upon heating to 1100 K, new peaks appear in the HREELS spectra alongside the C_{60} features, and after the 1200 K anneal these new peaks at 252 and 740 cm^{-1} dominate the spectra. C_{60} fragmentation begins at 1200 K, as characterized by the loss of C_{60} features in the HREELS spectra and the appearance of a graphitic ring in LEED.

5. Conclusions

The major conclusions of this work can be stated as follows.

(1) Vibrational spectra from HREELS show strong interactions between C_{60} and Pt(111) that lead to charge transfer from Pt of about two electrons per C_{60} molecule for $\theta(C_{60})=0.3$ ML, and one electron per C_{60} molecule for $\theta(C_{60})=$ 1.0 ML. These charge transfer interactions are inhibited by alloying of Pt(111) with Sn to form the $(\sqrt{3}\times\sqrt{3})R30^\circ$ Sn/Pt(111) surface alloy.

(2) Ordered structures of C_{60} can be formed on Pt(111) by annealing multilayer C_{60} films to 900 K. However, Pt(111) catalyzes the graphitization of C_{60} beginning at 900 K, and so LEED reveals a large background intensity and a graphitic ring in addition to the ordered C_{60} domains. On Pt(111), complete graphitization of C_{60} occurs after annealing to 1000 K, but this is arrested on the $\sqrt{3}$ Sn/Pt(111) alloy at 900 K. Sn is dealloyed at high temperatures and stabilizes the ordered C_{60} monolayer until 1100 K, close to the fragmentation temperature of solid C_{60}.

(3) C_{60} chemically reacts with dealloyed Sn at 450–700 K, but the charge transfer per C_{60} molecule from Sn is small. The C(1s) core level in XPS shows a 0.3 eV shift to lower BE and about 15% of surface Sn shows a shift in the Sn(3d) levels of 1.2 eV to higher BE. Reaction causes a rise in intensity of the unpolarized Raman-active $A_g(2)$ mode in HREELS, and this arises from reducing the icosahedral symmetry of the C_{60} molecule because of Sn–C_{60} bonding.

Acknowledgements

We acknowledge support of this work by the Divisions of Chemistry and Materials Research of the National Science Foundation (NSF).

References

[1] P. Dumas, M. Gruyters, P. Rudolf, Y. He, L.M. Yu, G. Gensterblum, R. Caudano, Y.J. Chabal, Surf. Sci. 368 (1996) 330.
[2] J. Schmidt, M.R.C. Hunt, P. Miao, R.E. Palmer, Phys. Rev. B 56 (1997) 9918.
[3] A.F. Hebard, O. Zhou, Q. Zhong, R.M. Fleming, R.C. Haddon, Thin Solid Films 257 (1995) 147.
[4] A.A. Lucas, J. Phys. Chem. Solids 53 (1992) 1415.
[5] H. He, N. Swami, B.E. Koel, Thin Solid Films, submitted for publication.
[6] K. Rikitake, T. Akiyama, W. Takashima, K. Kaneto, Synth. Met. 86 (1997) 2357.
[7] A.F. Hebard, R. Ruel, C.B. Eom, Phys. Rev. B 54 (1996) 14052.
[8] G.P. Kochanski, A.F. Hebard, R.C. Haddon, Science 255 (1992) 154.
[9] N. Swami, Y. You, M.E. Thompson, B.E. Koel, J. Vac. Sci. Technol. A: 16 (1998) 2395.
[10] R.C. Haddon, A.S. Perel, R.C. Morris, T.T.M. Palstra, A.F. Hebard, R.M. Fleming, Appl. Phys. Lett. 67 (1995) 121.

[11] S. Modesti, S. Cerasari, P. Rudolf, Phys. Rev. Lett. 71 (1993) 2469.
[12] A.J. Maxwell, P.A. Bruhwiler, A. Nilsson, M. Martensson, P. Rudolf, Phys. Rev. B 49 (1994) 10717.
[13] A. Sellidj, B.E. Koel, J. Phys. Chem. 97 (1993) 10076.
[14] S. Suto, K. Sakamoto, T. Wakita, C. Hu, A. Kasuya, Phys. Rev. B 56 (1997) 7439.
[15] X.D. Zhang, W.B. Zhao, K. Wu, Z.Y. Ye, J.L. Zhang, C.Y. Li, D.L. Yin, Z.N. Gu, X.H. Zhou, Z.X. Jin, Chem. Phys. Lett. 228 (1994) 100.
[16] W. Zhao, K. Luo, J. Cheng, C. Li, D. Yin, Z. Gu, X. Zhou, Z. Jin, J. Phys.: Condensed Matter 4 (1992) L513.
[17] N. Swami, H. He, B.E. Koel, Phys. Rev. B 59 (1999), in press.
[18] C. Cepek, A. Goldoni, S. Modesti, Phys. Rev. B 53 (1996) 7466.
[19] S.H. Overbury, D.R. Mullins, M.T. Paffett, B.E. Koel, Surf. Sci. 254 (1991) 45.
[20] M.T. Paffett, S.C. Gebhard, R.G. Windham, B.E. Koel, J. Phys. Chem. 94 (1990) 6831.
[21] Z. Gu, J. Qian, J. Zhaoxia, Z. Xihuang, Solid State Commun. 82 (1992) 167.
[22] W. Zhao, Y. Li, L. Chen, Z. Liu, Y. Huang, Z. Zhao, Solid State Commun. 92 (1994) 313.
[23] W. Zhao, K. Luo, J. Chen, J. Zhang, C. Li, D. Yin, Z. Gu, X. Zhou, Z. Jin, Solid State Commun. 83 (1992) 853.
[24] D. Junzhou, X. Kun, Y. Jun, L. Fengqin, L. Sihua, W. Zuquan, W. Sicheng, Solid State Commun. 84 (1992) 793.
[25] W. Zhao, T.N. Zhao, J.J. Yue, L.Q. Chen, J.Q. Liu, Solid State Commun. 84 (1992) 323.
[26] G.K. Wertheim, D.N.E. Buchanan, A. Chaban, J.E. Rowe, Solid State Commun. 83 (1992) 785.
[27] E. Kolodney, B. Tsipinyuk, A. Budrevich, J. Chem. Phys. 100 (1994) 8452.
[28] M.R. Stetzer, P.A. Heiney, J.E. Fischer, A.R. McGhie, Phys. Rev. B 55 (1997) 127.
[29] C.S. Sundar, A. Bharathi, Y. Hariharan, J. Janaki, V. Sankara Sastry, T.S. Radhakrishnan, Solid State Commun. 84 (1992) 823.
[30] M.J. Rice, H. Choi, Phys. Rev. B 45 (1992) 10173.
[31] T. Pichler, R. Winkler, H. Kuzmany, Phys. Rev. B 49 (1994) 15879.
[32] M.R.C. Hunt, S. Modesti, P. Rudolf, R.E. Palmer, Phys. Rev. B 51 (1995) 10039.
[33] G. Gensterblum, L. Yu, J.J. Pireaux, P.A. Thiry, R. Caudano, P.H. Lambin, A.A. Lucas, W. Kratschmer, J.E. Fischer, J. Phys. Chem. Solids 53 (1992) 1427.
[34] J.H. Weaver, J.L. Martins, T. Komeda, Y. Chen, T.R. Ohno, G.H. Kroll, N. Troullier, R.E. Haufler, R.E. Smalley, Phys. Rev. Lett. 66 (1991) 1741.
[35] J.E. Rowe, P. Rudolf, L.H. Tjeng, R.A. Malic, G. Meigs, C.T. Chen, J. Chen, E.W. Plummer, Int. J. Mod. Phys. B:, (1992)
[36] D.M. Poirier, T.R. Ohno, G.H. Kroll, Y. Chen, P.J. Benning, J.H. Weaver, L.P.F. Chibante, R.E. Smalley, Science 253 (1991) 646.
[37] Y. Li, M.R. Voss, N. Swami, Y. Tsai, B.E. Koel, Phys. Rev. B 56 (1997) 1.
[38] Handbook of X-Ray Photoelectron Spectroscopy, Perkin–Elmer Corporation, 1978.
[39] M.T. Paffett, S.C. Gebhard, R.G. Windham, B.E. Koel, Surf. Sci. 223 (1989) 449.
[40] C. Xu, B.E. Koel, Surf. Sci. 310 (1994) 198.
[41] G.K. Wertheim, D.N.E. Buchanan, Solid State Commun. 88 (1993) 97.
[42] P.W. Atkins, Physical Chemistry, 5th edition, Freeman, New York, 1994.
[43] H. Nagashima, A. Nakaoka, Y. Saito, M. Kato, T. Kawanishi, K. Itoh, J. Chem. Soc. Chem. Commun. (1992) 377.
[44] L. Norin, U. Jansson, C. Dyer, P. Jacobsson, S. McGinnis, Chem. Mater. 10 (1998) 1184.
[45] A.M. Rao, P. Zhou, K. Wang, G.T. Hager, J.M. Holden, Y. Wang, W.T. Lee, X. Bi, P.C. Eklund, D.S. Cornett, M.A. Duncan, I.J. Amster, Science 259 (1993) 955.
[46] P.C. Eklund, A.M. Rao, P. Zhou, Y. Wang, K. Wang, G.T. Hager, J.M. Holden, Mater. Sci. Eng. B 19 (1993) 154.
[47] A. Ito, T. Morikawa, T. Takahashi, Chem. Phys. Lett. 211 (1993) 333.